LUF7244 plus Dofetilide Rescues Aberrant K$_v$11.1 Trafficking and Produces Functional I$_{Kv11.1}$

Muge Qile,[1] Yuan Ji,[1] Tyona D. Golden, Marien J.C. Houtman, Fee Romunde, Doreth Fransen, Willem B. van Ham, Ad P. IJzerman, Craig T. January, Laura H. Heitman, Anna Stary-Weinzinger, Brian P. Delisle, and ⓘ Marcel A.G. van der Heyden

Department of Medical Physiology, University Medical Center Utrecht, Utrecht, The Netherlands (M.Q., Y.J., M.J.C.H., F.R., D.F., W.B.H., M.A.G.H.); Department of Physiology, University of Kentucky, Lexington, Kentucky (T.D.G., B.P.D.); Department of Pharmacology and Toxicology, University of Vienna, Vienna, Austria (W.B.H., A.S.-W.); Leiden Academic Centre for Drug Research, Division of Drug Discovery and Safety, Leiden, The Netherlands (A.P.I., L.H.H.); and Department of Medicine, University of Wisconsin, Madison, Wisconsin (C.T.J.)

ABSTRACT

Voltage-gated potassium 11.1 (K$_v$11.1) channels play a critical role in repolarization of cardiomyocytes during the cardiac action potential (AP). Drug-mediated K$_v$11.1 blockade results in AP prolongation, which poses an increased risk of sudden cardiac death. Many drugs, like pentamidine, interfere with normal K$_v$11.1 forward trafficking and thus reduce functional K$_v$11.1 channel densities. Although class III antiarrhythmics, e.g., dofetilide, rescue congenital and acquired forward trafficking defects, this is of little use because of their simultaneous acute channel blocking effect. We aimed to test the ability of a combination of dofetilide plus LUF7244, a K$_v$11.1 allosteric modulator/activator, to rescue K$_v$11.1 trafficking and produce functional K$_v$11.1 current. LUF7244 treatment by itself did not disturb or rescue wild type (WT) or G601S-K$_v$11.1 trafficking, as shown by Western blot and immunofluorescence microcopy analysis. Pentamidine-decreased maturation of WT K$_v$11.1 levels was rescued by 10 μM dofetilide or 10 μM dofetilide + 5 μM LUF7244. In trafficking defective G601S-K$_v$11.1 cells, dofetilide (10 μM) or dofetilide + LUF7244 (10 + 5 μM) also restored K$_v$11.1 trafficking, as demonstrated by Western blot and immunofluorescence microscopy. LUF7244 (10 μM) increased I$_{Kv11.1}$ despite the presence of dofetilide (1 μM) in WT K$_v$11.1 cells. In G601S-expressing cells, long-term treatment (24–48 hour) with LUF7244 (10 μM) and dofetilide (1 μM) increased I$_{Kv11.1}$ compared with nontreated or acutely treated cells. We conclude that dofetilide plus LUF7244 rescues K$_v$11.1 trafficking and produces functional I$_{Kv11.1}$. Thus, combined administration of LUF7244 and an I$_{Kv11.1}$ trafficking corrector could serve as a new pharmacological therapy of both congenital and drug-induced K$_v$11.1 trafficking defects.

SIGNIFICANCE STATEMENT

Decreased levels of functional K$_v$11.1 potassium channel at the plasma membrane of cardiomyocytes prolongs action potential repolarization, which associates with cardiac arrhythmia. Defective forward trafficking of K$_v$11.1 channel protein is an important factor in acquired and congenital long QT syndrome. LUF7244 as a negative allosteric modulator/activator in combination with dofetilide corrected both congenital and acquired K$_v$11.1 trafficking defects, resulting in functional K$_v$11.1 current.

Introduction

Human K$_v$11.1 potassium ion channels (also known as human *ether-a-go-go* related gene (hERG) channels) stand at the basis of the rapidly activating delayed rectifier current (I$_{Kr}$), which is involved in phase three repolarization of the action potential (AP) in working cardiomyocytes (Vandenberg et al., 2012). Interference with normal I$_{Kr}$ function can either shorten (gain-of-function) or prolong (loss-of-function) the process of ventricular repolarization, as evident from QT-shortening or lengthening, respectively, on the ECG (Vandenberg et al., 2012). I$_{Kr}$ inhibition in humans, e.g., by the class III agent dofetilide, is associated with life-threatening ventricular arrhythmias (Torp-Pedersen et al., 1999). Fundamentally different mechanisms of I$_{Kr}$ inhibition have been identified: 1) direct inhibition of potassium flow through the channel and 2) decreased plasma membrane expression of channel proteins, which both can result from mutations (de novo or congenital) or environmental factors (acquired, mostly drug-induced) (Sanguinetti and Tristani-Firouzi, 2006; De Git et al., 2013). For these reasons, cardiac

ABBREVIATIONS: AP, action potential; APD, action potential duration; cryo-EM, cryogenic electron microscopy; DMEM, Dulbecco's modified eagle medium; EAD, early after depolarization; HEK, human embryonic kidney cells; hERG, the human *ether-a-go-go* related gene encoded channel protein; I$_{KV}$, current conducted by voltage-gated potassium channels; K$_v$, voltage-gated potassium channels; LQT2, the second most common long QT syndrome; POPC, phosphatidylcholines; PMSF, phenylmethylsulfonyl fluoride; WT, wild type.

safety assessment of new chemical entities and preclinical drugs still has a strong focus on $K_v11.1$ channel function (Bossu et al., 2016) and mainly aims at detection of (semi) acute pore block. Interestingly, the vast majority (approximately 90% of 167 tested) of congenital $K_v11.1$ loss-of-function missense mutations result in trafficking defects as a cause of I_{Kr} impairment (Anderson et al., 2006, 2014). For example, the G601S missense mutation in $K_v11.1$, located in the S5-pore helix linker, results in reduced expression of functional I_{Kr}, leading to hypomorphic LQT2 (the second most common long QT syndrome) (Ficker et al., 2002). Also, a number of drugs (>40% of 100 tested) limit expression of $K_v11.1$ at the plasma membrane by inhibiting its forward trafficking, with or without concomitant pore block (Wible et al., 2005). The anti-trypanosomiasis/leishmaniasis drug pentamidine is currently used as a $K_v11.1$ trafficking inhibitor without acute channel inhibition (Cordes et al., 2005; Kuryshev et al., 2005; Nalos et al., 2011; Himmel 2013; Varkevisser et al., 2013a,b; Obergrussberger et al., 2016). Pentamidine inhibits $K_v11.1$ forward trafficking at the level of endoplasmic reticulum exit in a process that involves the high-affinity drug binding site F656 (Dennis et al., 2012). As a result, cells mainly express intracellularly localized core-glycosylated $K_v11.1$ with an apparent molecular mass of 135 kDa.

High-affinity $K_v11.1$ pore blockers such as E4031, dofetilide, cisapride, and astemizole are able to rescue forward trafficking defects caused by either mutations or drugs (Zhou et al., 1999; Ficker et al., 2002; Varkevisser et al., 2013a; Yan et al., 2015). This will result in $K_v11.1$ maturation, seen as a fully glycosylated protein with an apparent molecular mass weight of 155 kDa. The underlying mechanisms have not been clarified completely thus far, although it is found that channel inhibition potency correlates with rescue efficacy and that drug-channel interactions via high-affinity binding sites are essential (Ficker et al., 2002; Rajamani et al., 2002; Dennis et al., 2012; Yan et al., 2015). Furthermore, EC_{50} values for rescue are generally much higher than IC_{50} values for acute pore block (e.g., astemizole, IC_{50} = 6–13 nM; EC_{50} for rescue = 335 ± 33 nM with 10 μM pentamidine) (Ficker et al., 2002; Dennis et al., 2012). Therefore, this strategy will not result in rescue of I_{Kr} function as long as the high-affinity blocker remains present, whereas its withdrawal will not resolve the underlying trafficking defects. Activators and negative allosteric modulators of $K_v11.1$ have been developed as a strategy to counteract undesired I_{Kr} blockade and thus potentially could "save" numerous (pre)clinical drugs with proven I_{Kr} liability (Yu et al., 2014, 2016; Sala et al., 2016; Qile et al., 2019). Allosteric modulators interact with the $K_v11.1$ channel at a site different than that used by the high-affinity inhibitors and thereby modulate binding affinities for the canonical binding site of the latter. Activators interact with $K_v11.1$ at various sites (Sanguinetti, 2014), and some share overlapping high-affinity molecular determinants (Casis et al., 2006; Perry et al., 2007; Garg et al., 2013) with classic pore blockers. We have developed the negative allosteric modulator/activator LUF7244, which indeed is able to counteract drug-induced AP prolongation and proarrhythmia in vitro (Yu et al., 2015, 2016) and drug-induced ventricular arrhythmia in vivo (Qile et al., 2019). Specifically, application of 10 μM LUF7244 decreased the affinity of $K_v11.1$ for cisapride, astemizole, dofetilide, and sertindole by 4.0-, 3.8-, 3.2-, and 2.2-fold, respectively (Yu et al., 2016). We hypothesized that LUF7244 would not interfere in $K_v11.1$ trafficking by itself and would also not interfere in dofetilide-mediated rescue of defective forward trafficking, but it maintains its ability to increase I_{Kr} in the presence of dofetilide.

Materials and Methods

Chemicals. LUF7244 was custom synthesized at the Division of Drug Discovery and Safety, Leiden Academic Centre for Drug Research, Leiden University, The Netherlands, as described earlier (Yu et al., 2016), and was dissolved in DMSO at 100 mM. Dofetilide was purchased from Sigma-Aldrich (Zwijndrecht, The Netherlands) and dissolved at 10 mM in DMSO. E4031 was dissolved in DMSO at 1 mM. Pentamidine-isethionate (Pentacarinat 300; Sanofi Aventis, Gouda, The Netherlands) was dissolved in water to provide a stock solution of 100 mM. All compounds were sterilized by filtration (0.22 μm), aliquoted, and stored at −20°C until use.

Molecular Modeling. Compounds LUF7244 and dofetilide were docked into the hERG cryogenic electron microscopy (cryo-EM) structure (Protein Data Bank code: 5va1, Wang and Mackinnon, 2017) using the GOLD software v.5.6.2. (Jones et al., 1997), essentially as described before (Qile et al., 2019). Two scoring functions, ChemPLP and Goldscore, were used, and 100 poses were collected per run with 125.000 Gold algorithm operations. The top 15 scoring poses each were analyzed using PyMol 1.7.2 (Schrödinger, 2015).

Molecular Dynamics Simulations. Simulations were essentially performed as described earlier (Qile et al., 2019) with a few small modifications. The $K_v11.1$ hERG structure was embedded in a phosphatidylcholines bilayer and solvated with transferable intermolecular potential with 3 points water using the CHARMM-GUI (Jo et al., 2008). KCl (150 mM) was added to the system, and potassium ions in the selectivity filter were placed at sites S0, S2, and S4, with water molecules at sites S1 and S3. Steepest descent energy minimization, followed by 2 nanoseconds of equilibration and 50 nanoseconds of production runs, were performed using GROMACS v.5.1.2 (Abraham et al., 2015) and the charmm36 force field (Vanommeslaeghe et al., 2010). Electrostatics were modeled using particle mesh Ewald (Darden et al., 1993), and linear constraint solver was used to constrain H-bonds (Hess et al., 1997). V-rescale (Bussi et al., 2007) was used to keep the temperature at 310 K, and semi-isotropic pressure coupling was done using the Parrinello-Rahman barostat (Parrinello and Rahman, 1981).

Cells. Human embryonic kidney (HEK)-hERG cells, which is the HEK293T cell line stably expressing human $K_v11.1$ protein, and hERG-G601S cells (HEK293T cell line stably expressing forward trafficking–deficient $K_v11.1$ protein) were cultured in Dulbecco's modified Eagle Medium (DMEM) (Gibco-FisherScientific, Landsmeer, The Netherlands) supplemented with 10% fetal calf serum (Sigma-Aldrich), 2 mM L-glutamine, 50 U·ml^{-1} penicillin, and 50 μg·ml^{-1} streptomycin (all three; Lonza, Breda, the Netherlands) as described before (Varkevisser et al., 2013a).

Patch-Clamp Electrophysiology. HEK-hERG and hERG-G601S cells were grown on Ø12-mm glass cover slips coated with poly-L-lysine (Sigma-Aldrich, German) and placed in a perfusion chamber (Cell Microcontrols, Norfolk, VA). Functional analyses were done by using a standard whole-cell patch-clamp technique on HEK293T cells stably expressing wild type (WT)- or G601S-$K_v11.1$ channels. The external solution contained (mM) 137 NaCl, 4 KCl, 1.8 CaCl$_2$, 1 MgCl$_2$, 10 glucose, and 10 HEPES (pH 7.4 adjusted with NaOH), and the internal pipette solution contained (mM) 130 KCl, 1 MgCl$_2$, 5 EGTA, 5 MgATP, and 10 HEPES (pH 7.2 adjusted with KOH). An Axopatch-200B patch-clamp amplifier (Axon Instruments, Union City, CA) was used to measure macroscopic currents and cell capacitance. The pipette resistances were 1–3 MΩ, and series resistance was compensated up to 90%. The pCLAMP 10 software (Axon Instruments) was used to generate the different voltage protocols, to acquire current signals, and for data analyses. We determined the

impact that dofetilide and LUF7244 had on K$_v$11.1 currents compared with control by applying step-like pulses from -80 to $+60$ mV in $+10$-mV increments for 5 seconds, followed by a "tail" pulse to -50 mV for 5 seconds. The maximal I$_{Kv11.1}$ measured during the tail pulse was plotted as a function of the step-pulse potential to generate the corresponding I–V relations.

Western Blot. Cell lysates were prepared in buffer D [20 mM HEPES, 125 mM NaCl, 10% glycerol, 1 mM EGTA, 1 mM dithiothreitol, 1 mM EDTA, and 1% Triton X-100 (pH 7.6)] supplemented with 1 mM phenylmethylsulfonyl flouride (PMSF) and 10 μg·ml^{-1} aprotinin. Protein lysate (25 μg) was mixed with Laemmli sample buffer, separated by 7% SDS-PAGE, and blotted onto a nitrocellulose membrane. Ponceau staining was used to reveal equal protein loading and subsequent quantification. Blots were blocked with 5% Protifar dissolved in Tris-buffered saline/Tween 20 [20 mM Tris-HCl (pH 8.0), 150 mM NaCl, 0.05% Tween-20 (v/v)] for 1 hour at room temperature. K$_v$11.1 protein was detected by polyclonal anti-hK$_v$11.1 (human K$_v$11.1 channel) primary antibody (catalogue number APC-062, 1: 3000; Alomone Laboratories, Jerusalem, Israel) and peroxidase-conjugated anti-rabbit secondary antibody (1:10,000; Jackson Immun-Research Laboratories Inc., West Baltimore Pike West Grove, PA). Final detection was performed using a standard enhanced chemiluminescent procedure (GE Lifescience, Marlborough, MA) with ChemiDocXRS system (BioRad Laboratories, Veenendaal, The Netherlands). Quantification analysis was performed using ImageJ 1.48V software (National Institutes of Health).

Immunofluorescence Microscopy. HERG-G601S cells were grown on Ø15-mm cover slips, coated with poly-L-Lysine, and fixated with 3% paraformaldehyde dissolved in PBS containing 1 mM Ca^{2+} and 1 mM Mg^{2+} (pH 7.4) for 20 minutes. Permeabilization was performed with 0.5% Triton X-100 in PBS for 3 minutes, 50 mM glycine-PBS was used as a quenching agent, and cells were subsequently blocked with NET-gel [150 mM NaCl, 5 mM EDTA, 50 mM Tris-HCl, (pH 7.4), 0.05% Igepal, 0.25% gelatin, 0.02% NaN$_3$]. Then, the cells were incubated with polyclonal anti-hK$_v$11.1 (human K$_v$11.1 channel) (1:3000, APC-062; Alomone Laboratories) and anti–Pancadherin (1:800; Sigma-Aldrich, St Louis, MO) primary antibody overnight in NET-gel, followed by incubation with secondary antibody of anti-mouse Alexa488 (Thermofisher Scientific, Landsmeer, The Netherlands) and anti-rabbit Alexa568 (Thermofisher Scientific) for 2 hours.

The cover slips were mounted with Vectashield (Vector Laboratories Inc. Burlingame, CA), and fluorescent microscopy images were obtained using a Nikon ECLIPSE Ti2-E inverted microscope equipped with a ×60 oil immersion objective (numerical aperture 1.49) (CAIRN research, Faversham, UK). Excitation was performed with diode lasers (Omicron LuxX 488 nm, 200 mW for Alexa488 and an OBIS 561 nm, 100 mW for Alexa561). Colocalization between K$_v$11.1 and cadherin in cell extensions was quantified by determining Pearson's coefficient (r) with the Costes automated threshold method provided by the Coloc_2 plug-in for the ImageJ software (1.52p) using Fiji.

Statistics. All average values are expressed as means ± S.D., unless indicated otherwise. All statistical analyses were carried out by using SPSS version 21 and Graphpad Prism version 5. A difference was considered significant with $P < 0.05$. Differences among groups were evaluated using either one-way ANOVA with Dunnett's test for Western blot and immunofluorescence microscopy data or two-way ANOVA with Tukey's test for electrophysiology data. Post hoc tests were carried out only if F was significant and there was no variance in homogeneity.

Results

Docking and Molecular Dynamics Simulation–Based Prediction of Binding Mode of Dofetilide and Its Interaction with LUF7244. Overview representations of K$_v$11.1 channel interaction with dofetilide and LUF7244 at the structural level, as viewed from the extracellular side, are shown in Fig. 1, A and B. To investigate how LUF7244 might lower the channel's affinities for dofetilide (Yu et al., 2016), we compared two binding modes of dofetilide and LUF7244. Figure 1, C and D displays two alternative binding modes of dofetilide in the near–atomic resolution cryo-EM structure (3.4 Å) of the K$_v$11.1 K$^+$ channel, in agreement with experimental data: in the cavity (Fig. 1D), which is the classic assumed binding mode for blockers (Kamiya et al., 2006; Imai et al., 2009), or in the fenestrations sticking into the cavity (Fig. 1C), as suggested recently, based on hERG homology models (Saxena et al., 2016). Both binding modes can be recapitulated in docking studies to the cryo-EM structure, and the drug is stable in 50 nanoseconds of molecular dynamics (Fig. 1, G and H) in both sites. We have recently reported that LUF7244 might bind between the pore helices of two adjacent subunits, thereby stabilizing the conductive state of the channel (Qile et al., 2019). Comparison of the proposed binding modes of dofetilide with that of LUF7244 (Fig. 1, E and F) suggests that the allosteric negative inhibitor/activator could prevent the inhibitor from binding to the fenestration site (Fig. 1E), whereas there is almost no overlap when dofetilide is bound to the central cavity (Fig. 1F).

LUF7244 Has No Effect on K$_v$11.1 Forward Trafficking and Does Not Interfere in Dofetilide-Mediated Rescue of Pentamidine-Induced Trafficking Defects. Application of LUF7244 (0.05, 0.1, 1, 3, and 5μM) for 48 hours did not obviously affect the K$_v$11.1 ratio of mature/immature protein as shown in Fig. 2A. We demonstrated earlier that dofetilide rescues pentamidine-induced K$_v$11.1 forward trafficking defects (Varkevisser et al., 2013a). To determine whether LUF7244 can restore mature K$_v$11.1 expression, different concentrations of LUF7244 were applied to HEK-hERG cells in the continuous presence of 10 μM pentamidine. However, treatment with LUF7244 up to 5 μM did not restore mature K$_v$11.1 protein levels (Fig. 2B).

Because LUF7244 by itself could not restore normal forward K$_v$11.1 channel trafficking and was found to counteract dofetilide-mediated I$_{Kr}$ blockade (Qile et al., 2019), we questioned whether LUF7244 would influence dofetilide-mediated rescue of pentamidine-induced trafficking defects. To test this hypothesis, the same dose range of LUF7244 was applied in combination with 1 μM dofetilide and 10 μM pentamidine for 48 hours. Interestingly, pentamidine decreased mature WT K$_v$11.1 protein [0.24 ± 0.07 vs. 0.54 ± 0.11 (control)], which was rescued by 1 μM dofetilide (0.44 ± 0.09 vs. 0.24 ± 0.07) and also by the combination of 1 μM dofetilide and 5 μM LUF7244 (0.45 ± 0.10 vs. 0.24 ± 0.07) (Fig. 2C). All the separate mature or immature K$_v$11.1 protein expression levels, quantified from the same blots, are shown in the right panel.

LUF7244 and Dofetilide/E4031 Rescue G601S-K$_v$11.1 Maturation. To test the effects of LUF7244 on a congenital K$_v$11.1 loss-of-function missense mutation that results in defective forward trafficking, we coapplied five different concentrations of LUF7244 and 1 μM dofetilide on hERG-G601S cells. According to Western blot result, trafficking deficiency was observed, which means only 135 kDa coreglycosylated immature protein was detected (Fig. 3A). After 48 hours of administration of LUF7244 (0.05, 0.1, 1, 3, and 5 μM), mature K$_v$11.1 protein level was not changed compared with control (Fig. 3A), whereas application of 1 μM dofetilide
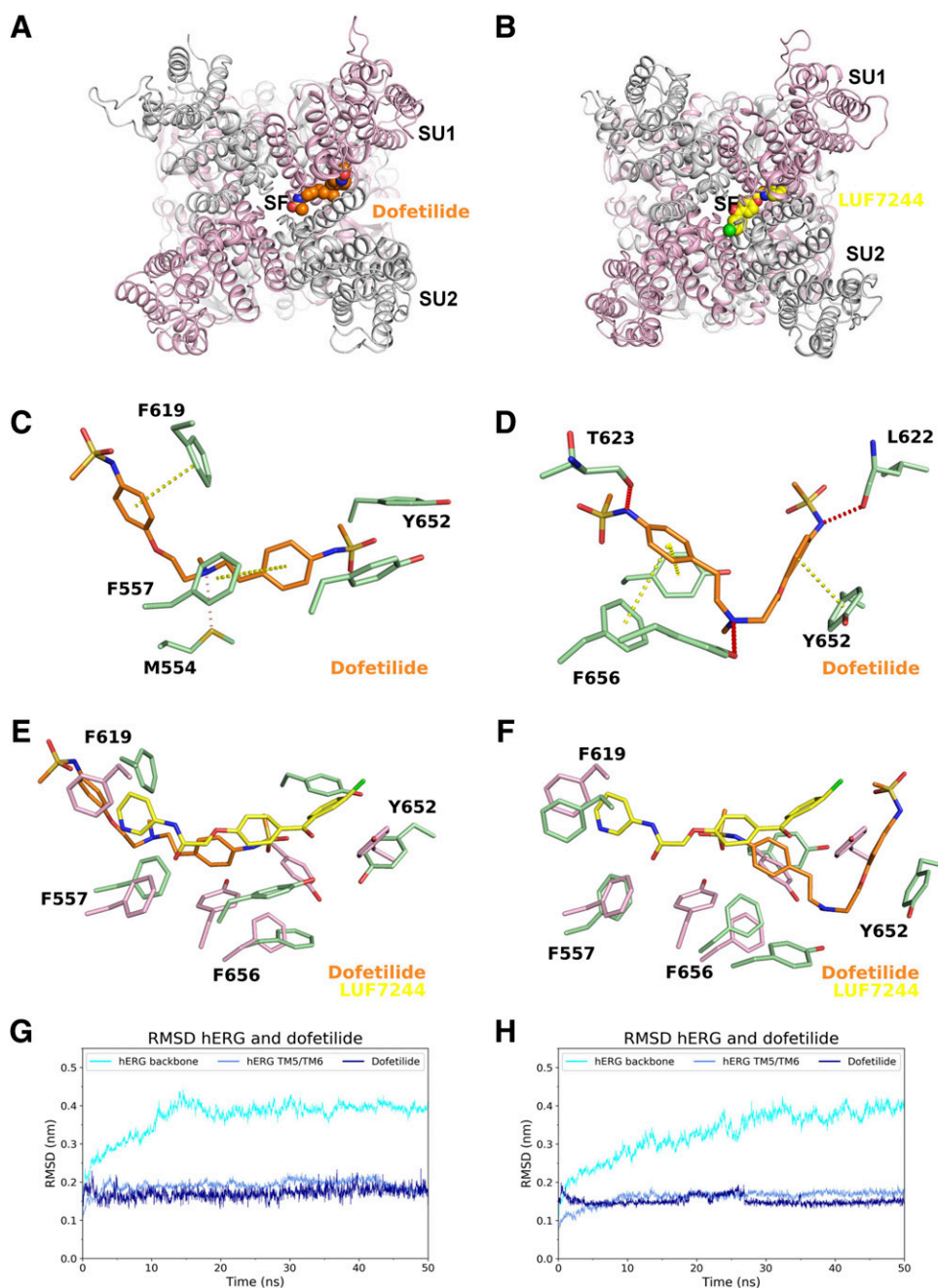
Fig. 1. Molecular dynamics simulation–based prediction of binding mode of dofetilide/LUF7244 and $K_v11.1$. (A) Overview of the hERG structure (top view), with bound dofetilide at the fenestration, shown as orange spheres. (B) Overview of the hERG structure (top view), with bound LUF7244. (C) Predicted binding modes for dofetilide at the fenestration. (D) Predicted "classic" binding mode for dofetilide in the inner cavity of hERG. Yellow dotted lines indicate putative π-π interactions; red dotted lines indicate H-bonds. (E and F) superposition of dofetilide binding modes, with predicted LUF7244 binding mode. (G and H) Root mean square deviation (RMSD) of $K_v11.1$ and dofetilide docked into the fenestration or cavity, respectively. SF, selectivity filter; SU, subunit; TM, transmembrane domain., subunit 1/2; TM5/6: the 5th/6th transmembrane domains.

greatly increased mature protein expression. Furthermore, 1 μM dofetilide combined with LUF7244 (0.05–5 μM) also resulted in expression of the fully glycosylated mature protein (Fig. 3B). To expand our findings to other I_{Kr} blockers, we used E4031. We applied 5 μM E4031 without or with LUF7244 (0.05, 0.1, 1, 3, and 5 μM) for 48 hours. Under all rescue conditions, the level of the 155 kDa fully glycosylated mature protein was increased (Fig. 3C), although not to the same extent as seen with dofetilide. The separate mature or immature $K_v11.1$ protein expression level can be found in the right panel.

Immunofluorescence staining was used to determine the subcellular localization of the G601S-$K_v11.1$ protein. In untreated control hERG-G601S cells, no $K_v11.1$ protein was detected at the cell membrane structures, such as membrane ruffles, in contrast to the transmembrane protein Cadherin (Fig. 4) (Pearson coefficient of colocalization $r = 0.20 \pm 0.35$, $n = 6$). After 24 hours of treatment with 10 μM dofetilide or 10 μM dofetilide + 3 μM LUF7244, normal trafficking was restored, as evidenced by plasma membrane expression of $K_v11.1$ in membrane ruffles, where it colocalized with Cadherin (Fig. 4) [$r = 0.85 \pm 0.08$ ($n = 6$) and 0.86 ± 0.06 ($n = 6$), respectively, both $P < 0.01$ vs. control or LUF7244]. LUF7244-only treatment yielded no rescue of forward trafficking ($r = 0.13 \pm 0.31$, n.s. vs. control). A lower concentration of LUF7244 was used to maintain intact cell structure in these experiments.

LUF7244 Increases $I_{Kv11.1}$ in the Presence of Dofetilide. Lastly, the impact of dofetilide and LUF7244 on $I_{Kv11.1}$ was determined (Fig. 5). The use of 10 μM LUF7244 in
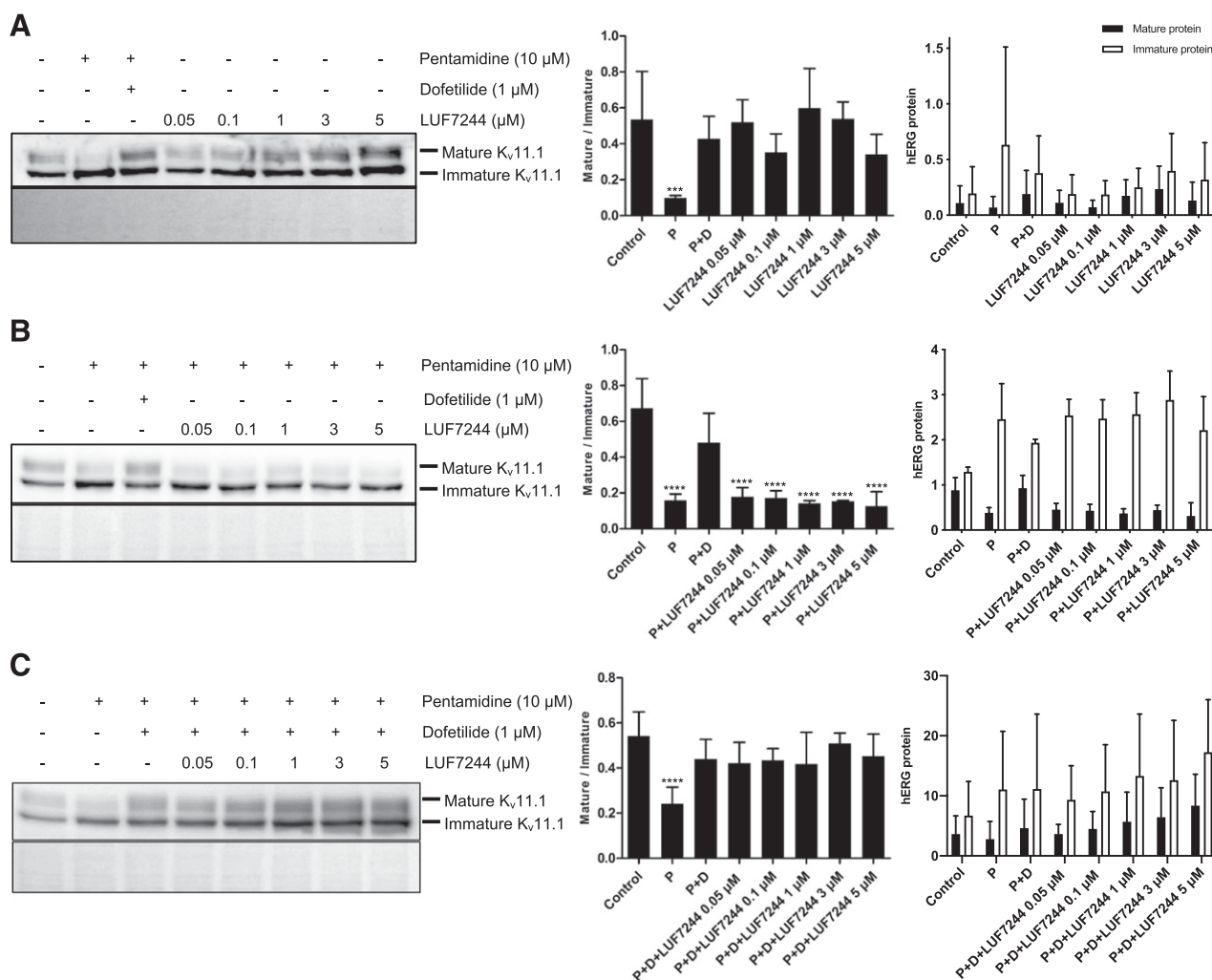
Fig. 2. LUF7244 alone has no effect on K$_v$11.1 trafficking and does not disturb dofetilide-mediated rescue of forward trafficking. (A) Western blot showing that treatment of pentamidine-exposed (10 μM, 48 hour) HEK-hERG cells with 1 μM dofetilide restored mature K$_v$11.1 expression. LUF7244 alone has no effect on K$_v$11.1 expression (n = 3). Mature (plasma membrane–expressed) and immature (intracellular) K$_v$11.1 Western blot signals are displayed in the left panel. Bar graphs in the middle depict the ratio of mature/immature K$_v$11.1 at different conditions. The right panel displays separate values for mature and immature K$_v$11.1. (B) LUF7244 does not rescue pentamidine-induced K$_v$11.1 trafficking defects (n = 3). (C) Combination of pentamidine, dofetilide, and LUF7244 restores K$_v$11.1 mature protein after 48 hours (n = 6). Total protein staining (Ponceau) was used as a loading control. ***P < 0.001; ****P < 0.0001 vs. control. Values are shown as means ± S.D. One-way ANOVA with Dunnett's test was applied for group comparison. P, pentamidine; D, dofetilide.

electrophysiology experiments is based on the strong I$_{Kv11.1}$ blockade effect of dofetilide. To counteract dofetilide's effect, we needed to use a relatively higher concentration than what we used in Western blot experiments. On the other hand, 10 μM LUF7244 was used in our previous work (Qile et al., 2019), which was based on the concentration that was used for its structurally similar compound ICA-105574.

Figure 5A shows representative current traces measured from cells expressing WT-K$_v$11.1 channel proteins in control conditions or with application of dofetilide (1 μM), LUF7244 (10 μM), or a combination to the extracellular recording solution as acute treatment. Cells were voltage-clamped at a holding potential of −80 mV and depolarized to voltages between −80 and 60 mV for 5 seconds to activate I$_{Kv11.1}$ (prepulse). The cells were then clamped to −50 mV for 5 seconds to record a tail current (test pulse). As shown for control cells in Fig. 5A, during depolarizing and tail pulses, an outward current was activated at voltages positive to −40 mV,

and the current amplitude of the I$_{Kv11.1}$ measured during the tail pulse increases with a maximum I$_{Kv11.1}$ current after depolarizing pulses to >10 mV. The peak tail I$_{Kv11.1}$ amplitude after repolarization was used to construct the activation curve shown in Fig. 5B. The activation curve measured for control cells shows that the threshold voltage for I$_{Kv11.1}$ activation is about −40 mV and that it is fully activated after voltage pulses to 10 mV. Dofetilide and LUF7244 dramatically alter the activation and kinetic properties of I$_{Kv11.1}$. The outward I$_{Kv11.1}$ measured during the depolarization and tail pulses is larger than control from −70 to 10 mV; there is a negative shift in the corresponding I–V relation; but I$_{Kv11.1}$ gets smaller after depolarizing pulses >0 mV. The changes in the I$_{Kv11.1}$ measured using this protocol in the presence of these drugs show complex changes consistent with both the activating properties of LUF7244 and blocking properties of dofetilide. The relevant LUF7244/dofetilide-alone control study is shown in Fig. 5.
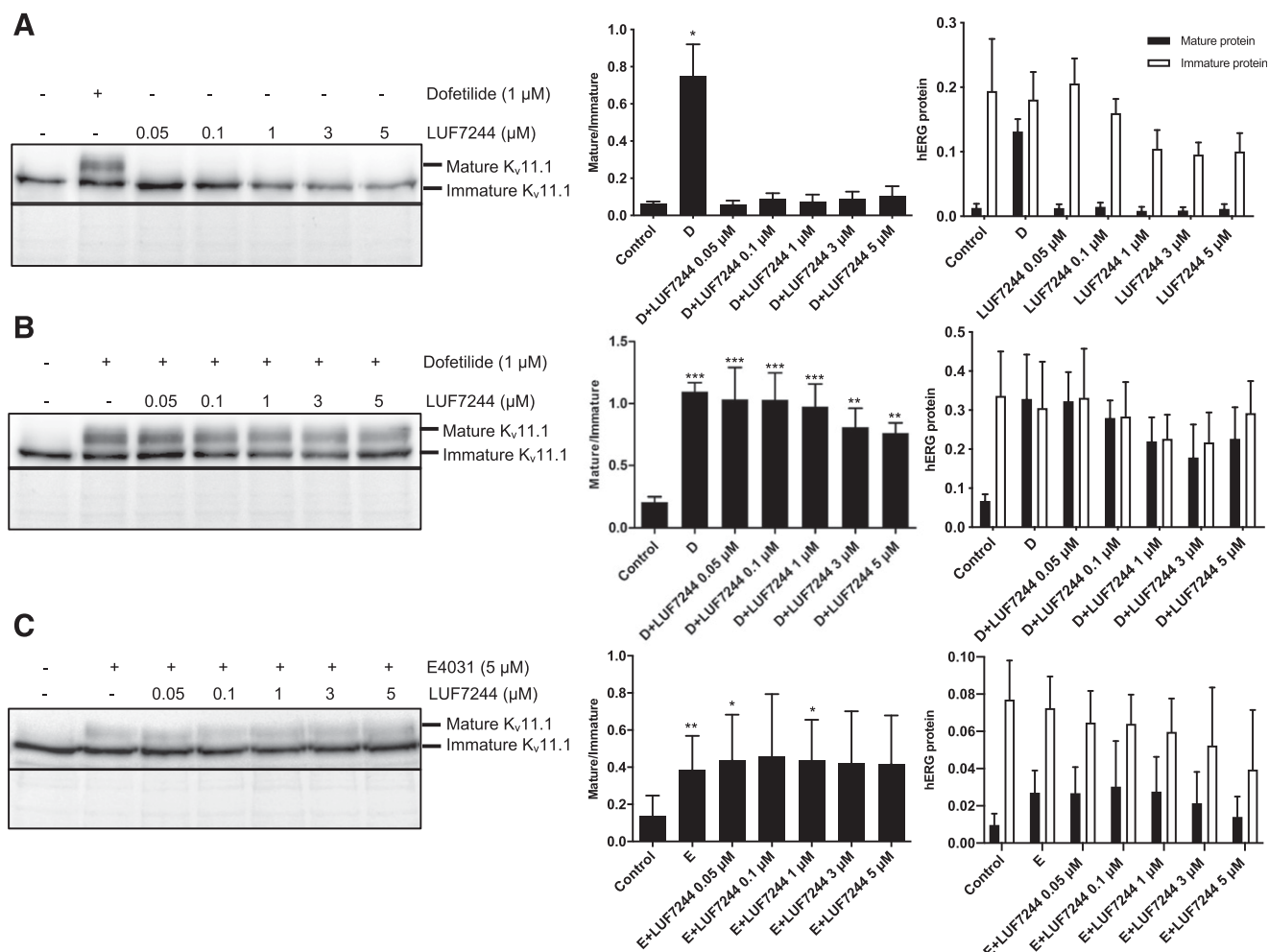
Fig. 3. LUF7244 combined with dofetilide or E4031 rescues trafficking-defective $K_v11.1$-G601S maturation. (A) Western blot analysis of equal amounts (25 μg) of total protein from $K_v11.1$-G601S cells. G601S cells only present a core-glycosylated immature protein of 135 kDa. Dofetilide restores expression of the full glycosylated mature protein after 48 hours. LUF7244 does not change the mature $K_v11.1$ protein levels compared with control ($n = 3$). (B) The combination of dofetilide and LUF7244 rescues mature $K_v11.1$ protein in G601S cells ($n = 3$). (C) Increased mature $K_v11.1$ levels in G601S cells treated with E4031 or E4031 + LUF7244 (48 hours) ($n = 6$). The right panel displays separate values for mature and immature $K_v11.1$. Total protein staining (Ponceau) was used as a loading control. $*P < 0.05$; $**P < 0.01$; $***P < 0.001$ vs. control. Values are shown as means ± S.D. One-way ANOVA with Dunnett's test was applied for group comparison. D, dofetilide; E, E4031.

Figure 6A shows representative current traces measured from cells expressing G601S-$K_v11.1$ channel proteins in control conditions and with acute or long-term application of dofetilide + LUF7244 or LUF7244 only to the extracellular recording solution. There was no statistical difference in $I_{Kv11.1}$ between the control conditions and acute application of dofetilide + LUF7244. Therefore, we tested the long-term effects of these drugs on $I_{Kv11.1}$. We incubated cells in dofetilide + LUF7244 for 24–48 hours and then recorded $I_{Kv11.1}$ from cells with these drugs in the extracellular recording solution. The mean I–V relations, based on peak tail $I_{Kv11.1}$ amplitude after repolarization, for cells expressing G601S-$K_v11.1$ channel proteins in the different conditions indicate that long-term dofetilide + LUF7244 treatment increased $I_{Kv11.1}$. Dofetilide-only treatment had a minimal effect (Fig. 6B), indicating the presence of only a few functional channels at the plasma membrane without prior pharmacological correction of trafficking. Interestingly, however, LUF7244-only treatment produced $I_{Kv11.1}$ under such conditions (Fig. 6). Compared with control cells, cells cultured and

recorded in dofetilide + LUF7244 increased $I_{Kv11.1}$ after prepulses from −40 to 60 mV ($P < 0.05$), and cells treated with LUF7244 increased $I_{Kv11.1}$ after prepulses from −80 to 60 mV ($P < 0.05$). Compared with cells recorded in dofetilide, cells cultured and recorded in dofetilide + LUF7244 increased $I_{Kv11.1}$ after prepulses from −40 to 60 mV ($P < 0.05$), and cells recorded in LUF7244 increased $I_{Kv11.1}$ after prepulses from −80 to 60 mV ($P < 0.05$). Compared with dofetilide + LUF7244, cells cultured and recorded in dofetilide + LUF7244 increased $I_{Kv11.1}$ after prepulses from −30 to 30 mV ($P < 0.05$), and cells recorded in LUF7244 increased $I_{Kv11.1}$ after prepulses from −80 to 60 mV ($P < 0.05$). Compared with cells cultured and recorded in LUF7244 cells, cells recorded in LUF7244 increased $I_{Kv11.1}$ after prepulses from −80 to 60 mV ($P < 0.05$).

Discussion

$K_v11.1$ activators and negative allosteric modulators use mechanistically different ways to increase or maintain normal
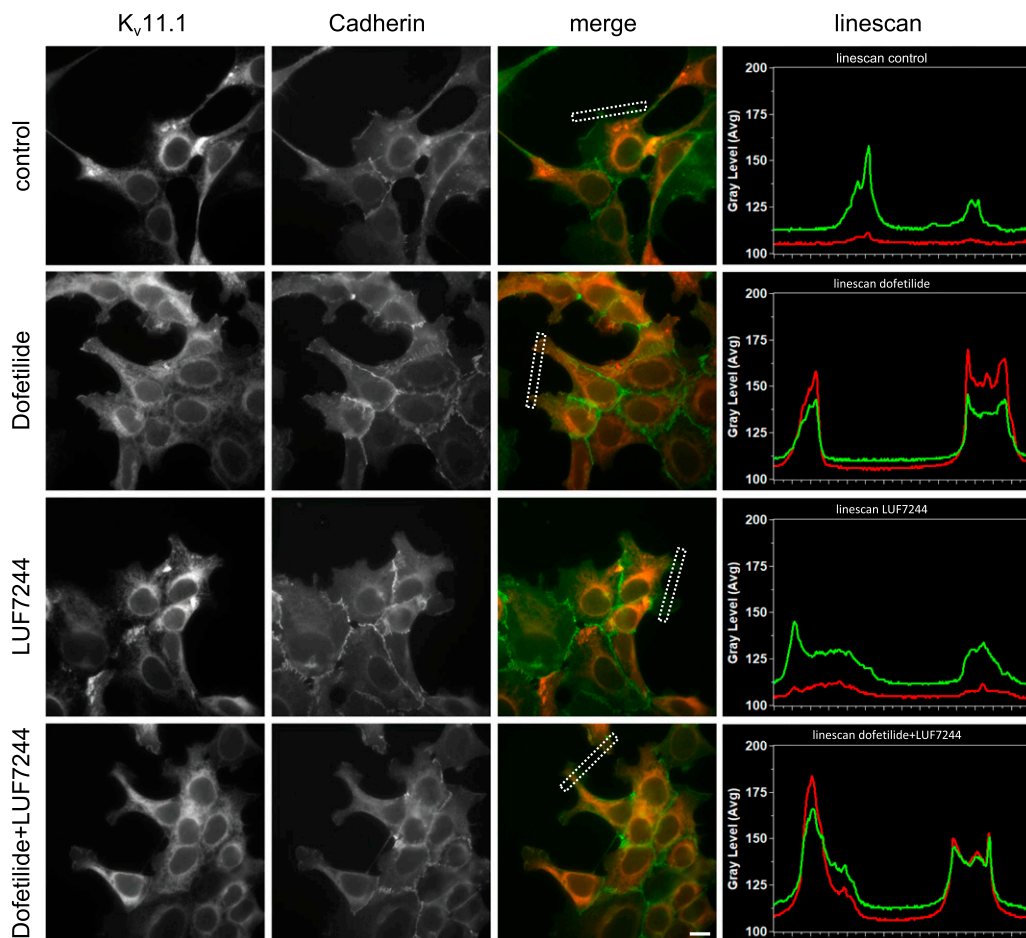
Fig. 4. G601S cells were either nontreated (control) or treated with 10 μM dofetilide, 3 μM LUF7244, or 10 μM dofetilide + 3 μM LUF for 24 hours. K$_v$11.1 channels were labeled (left column), along with Cadherin as a pseudomembrane marker (Cadherin). Line scans of selected regions at cell extensions (containing membrane ruffles) are indicated in the merged pictures by boxes. Results of the line scan recordings are given on the right panels. Scale bar, 10 μm.

I$_{Kr}$ levels in the presence of a K$_v$11.1 channel inhibitor. A number of compounds have been demonstrated as K$_v$11.1 activators (Perry et al., 2010). Activators influence gating kinetics and can, for example, slow down or remove inactivation and/or facilitate activation (Sanguinetti, 2014). K$_v$11.1 activators normally interact with a region distant from the inner cavity (Perry et al., 2010), but they can bind to several distinct sites of the channel (Perry et al., 2007; Guo et al., 2015; Gardner et al., 2017). Negative allosteric modulators decrease the binding affinity of I$_{Kr}$ blockers, either by increasing dissociation rates, lowering association rates, or both (Christopoulos et al., 2014). In our previous study, and also shown here, LUF7244 alone can dose dependently increase K$_v$11.1 current and reduce inactivation of K$_v$11.1 at higher concentration (Qile et al., 2019). In the current study, instead of the blockade effect of dofetilide, dofetilide + LUF7244 treatment led to a statistically significant increase in I$_{Kv11.1}$ level in HEK-hERG cells. In G601S cells, dofetilide + LUF7244 treatment increased (not statistically significantly) steady-state current as well. Furthermore, long-term exposure increased I$_{Kv11.1}$ continuously, which indicates that I$_{Kr}$ inhibitors' acute channel blockade could be reversed by LUF7244 and that its trafficking rescue characteristic might further functionally benefit K$_v$11.1 for long-term administration.

We observed a stronger I$_{Kv11.1}$ increase for G601S channels than for WT channels (Figs. 5 and 6), which could not be explained by methodological means. Although speculative, we can envision that, besides an effect on trafficking, the G601S mutation may result in increased binding affinity for LUF7244 or show subtly different channel kinetics in response to LUF7244 compared with WT. Whether these effects are mutation-specific are points for further investigation. Furthermore, the finding that LUF7244 can strongly activate the low amount of G601S channels that do reach the plasma membrane in cells not treated with dofetilide may shortcut the need for complete restoration of trafficking.

Modeling suggests that LUF7244 disrupts drug blocking at the fenestration via binding close to the protein-lipid interface (Fig. 1F). Drug binding to this site has recently been reported for ivabradine, a K$_v$11.1 blocker (Perissinotti et al., 2019) with low micromolar affinity. It has been reported that this drug interacts with lipid-facing residues in the fenestration, including F557 and F656, in a state-dependent manner. Even though dofetilide is unlikely to access the K$_v$11.1 cavity via this fenestration, as has been shown for the more lipophilic drug ivabradine, residue F557 has been shown to reduce binding affinity >50-fold when mutated to a leucine (Saxena et al., 2016). This suggests that this lipid-facing residue is
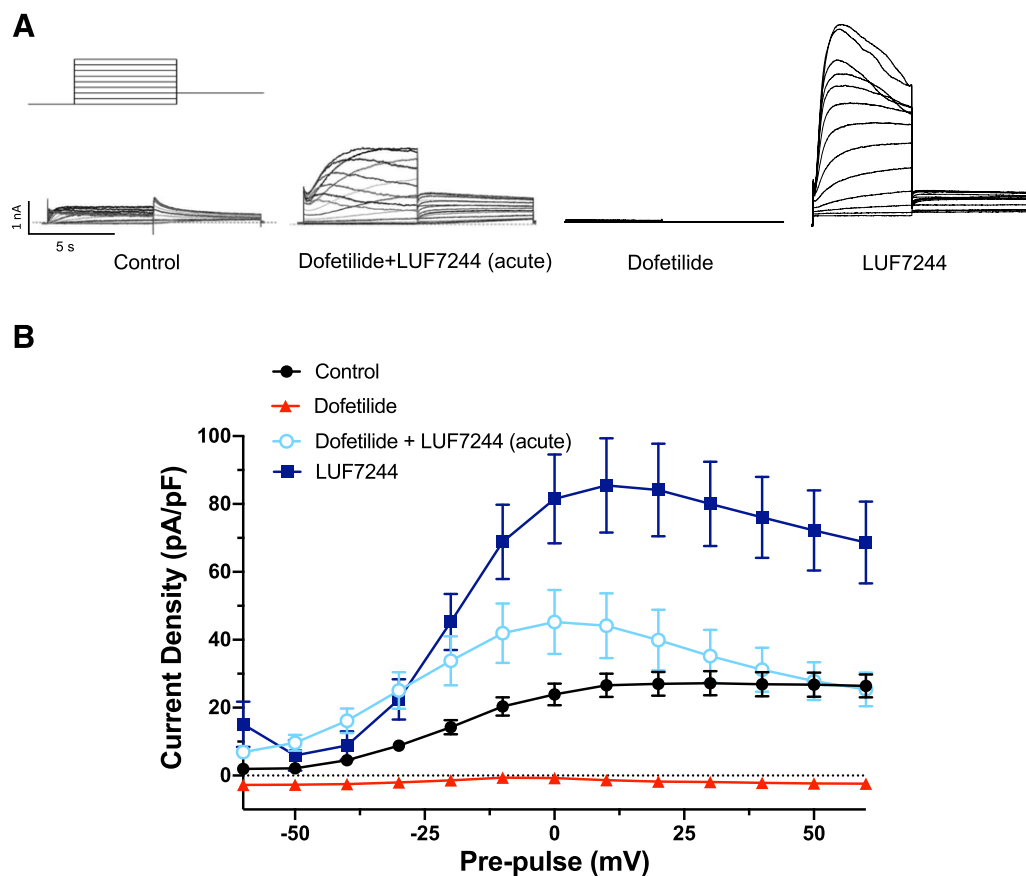
A

B

Fig. 5. LUF7244 combined with dofetilide acutely rescued $I_{Kv11.1}$ in HEK-hERG cells. (A) Shown are representative currents from cells expressing WT-$K_v11.1$ channel proteins using the voltage protocol in the inset. Cells were recorded in control conditions or in dofetilide + LUF7244 (acute application). In (B), shown are the mean I–V relations based on peak tail $I_{Kv11.1}$ amplitude after repolarization, recorded from cells expressing WT-$K_v11.1$ channel proteins. Cells were recorded in control conditions ($n = 10$) or in dofetilide + LUF7244 (acute) ($n = 10$). Data are shown as means ± S.E.M. Compared with control cells, cells recorded in dofetilide + LUF7244 increased $I_{Kv11.1}$ after prepulses from -70 to 10 mV ($P < 0.05$). Two-way ANOVA with Tukey's test was applied.

critical for high-affinity block of different hERG inhibitors. Our modeling proposes that LUF7244 could disrupt coupling between state-dependent dynamics of F557 and F656 and interfere with dofetilide binding to the fenestration (Fig. 1E). Given the impact of LUF7244 on inactivation, one plausible scenario would be that the negative allosteric inhibitor prevents dofetilide from binding or accessing the "high-affinity" inactivated state in the fenestration, but this will require further modeling of the inactivated state(s).

However, based on the current simulations of 50 nanoseconds, we cannot exclude that $K_v11.1$ has additional LUF7244 binding sites. Additional binding sites may explain the dual character of LUF7244 as a negative allosteric modulator (Yu et al., 2016) and activator (Qile et al., 2019, this study). Additional experimental analyses that may require in-depth NMR studies on drug-channel interaction are necessary to resolve this issue. The I_{Kr} activator ICA-105574 has structural similarities with LUF7244 and also has similar functional characteristics (Gerlach et al., 2010). It was shown that ICA-105574 enhanced $K_v11.1$ currents via a mechanism that seems to prevent or limit the inactivation gating process. Additionally, ICA-105574 dose dependently shortened the AP duration in isolated guinea pig ventricular cardiomyocytes. It also remarkably suppressed the $K_v11.1$ channel inhibitor

E4031-induced AP lengthening. In this perspective, it would be interesting to compare these two compounds with respect to the mechanism of action on $K_v11.1$ channels.

Besides, in view of its predicted binding site, LUF7244 by itself had no effects on $K_v11.1$ channel trafficking, and it neither inhibited pentamidine-associated trafficking defects nor affected dofetilide-mediated rescue. Previously, we demonstrated that pentamidine-induced $K_v11.1$ forward trafficking defects could be rescued by dofetilide and that both compounds may compete for the same binding site within the $K_v11.1$ channel (Varkevisser et al., 2013a). Defective $K_v11.1$ forward trafficking can be restored by a number of $K_v11.1$ inhibitors that stabilize the channel via binding to the inner pore, close to the selectivity filter (e.g., Perry et al., 2010; Varkevisser et al., 2013a). We demonstrated that dofetilide analogs with higher affinity tended to provide better rescue in $K_v11.1$ trafficking defects, whereas LUF7244 reduced the $K_v11.1$ channel affinity for dofetilide (Yu et al., 2016). Interestingly, in our current study, the combination of dofetilide and LUF7244 still rescued pentamidine-induced $K_v11.1$ trafficking defects. One possible reason may be that LUF7244 cannot completely reduce the binding of dofetilide to the trafficking-inhibited channels by which the capacity of dofetilide to rescue $K_v11.1$ trafficking remained. Another
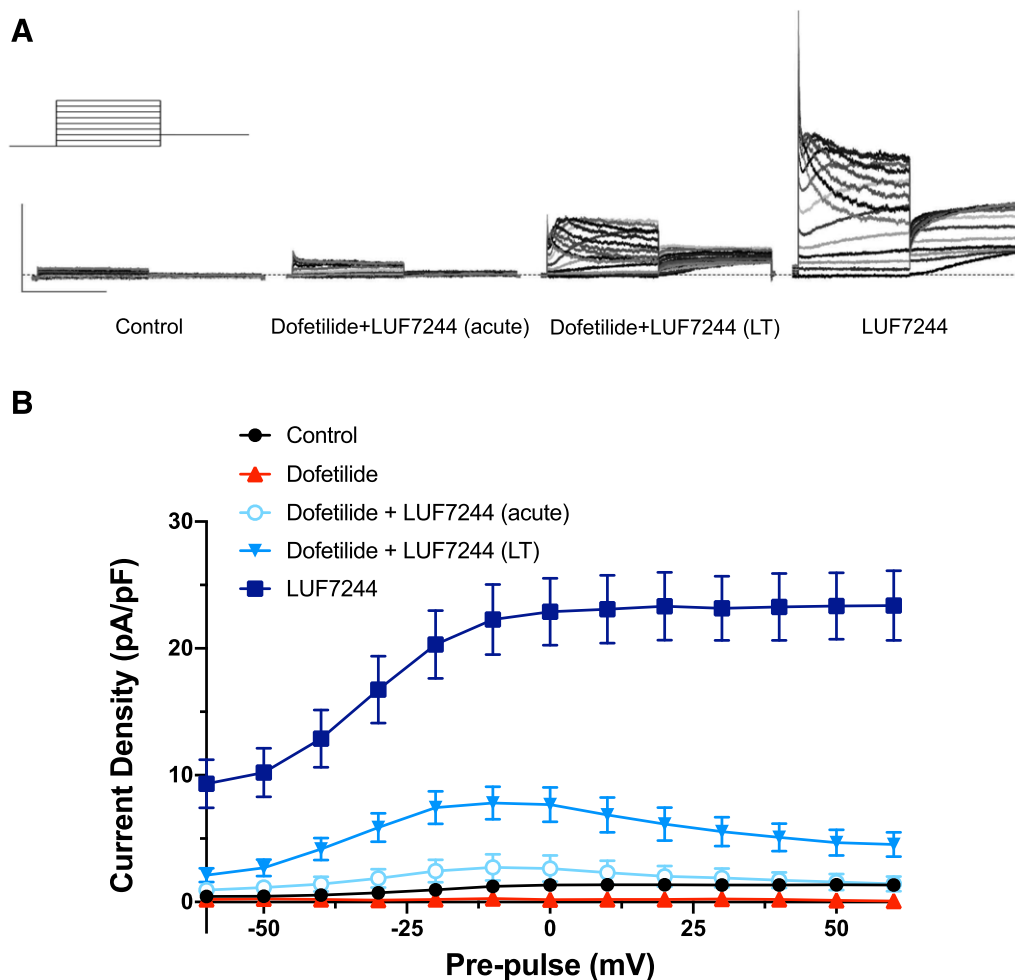
A

Control   Dofetilide+LUF7244 (acute)   Dofetilide+LUF7244 (LT)   LUF7244

B

Fig. 6. Long-term (24–48 hours) exposure of LUF7244 combined with dofetilide rescued I$_{Kv11.1}$ in G601S cells. (A) Shown are representative currents from cells expressing G601S-K$_v$11.1 channel proteins using the voltage protocol in the inset. Cells were recorded in control conditions, in dofetilide + LUF7244 (acute), in dofetilide + LUF7244 after being cultured long-term in dofetilide + LUF7244 (LT), or in LUF7244 (acute). (B) Shown are the mean I–V relations based on peak tail I$_{Kv11.1}$ amplitude after repolarization, recorded from cells expressing G601S-K$_v$11.1 channel proteins. Cells were recorded in control conditions ($n = 10$), in dofetilide ($n = 8$), in dofetilide + LUF7244 (acute) ($n = 10$), in dofetilide + LUF7244 after being cultured in dofetilide + LUF7244 for 24–48 hours (LT) ($n = 10$), or in LUF7244 ($n = 7$). Data are shown as means ± S.E.M. Two-way ANOVA with Tukey's test was applied.

possibility is the absence of LUF7244 binding to intracellularly localized, immature, and only core-glycosylated K$_v$11.1 channels. This may also explain 1) the absence of effects of LUF7244 on defective G601S trafficking, 2) the lack of interference of pentamidine-mediated trafficking defects by LUF7244, and 3) permitting dofetilide- and E4031-mediated rescue of K$_v$11.1 trafficking. Recent preliminary data indicate that dofetilide specifically binds to membrane preparations of G601S cells, which is in line with the observed trafficking rescue effect. It now has to be determined to which extent this binding is sensitive to LUF7244. We hypothesize that LUF7244 will certainly not completely inhibit dofetilide binding to intracellularly localized K$_v$11.1; otherwise, dofetilide + LUF7244 would not provide any rescue of maturation, membrane staining, and I$_{Kv11.1}$, as shown in the current manuscript.

Negative allosteric modulators and activators can be considered as therapeutic options to prevent drug-induced arrhythmia (Sanguinetti 2014; Yu et al., 2016). Recently, we have shown that LUF7244 suppressed astemizole-induced

early after depolarizations (EADs) andAP AP prolongation in neonatal rat ventricular myocytes (Yu et al., 2016). Additionally, LUF7244 pretreatment prevented the occurrence of astemizole-induced EADs, whereas LUF7244 per se did not shorten AP duration (APD) or strongly affect dispersion of APD$_{40}$ in neonatal rat ventricular myocytes at 10 μM (Yu Z et al., 2016). In contrast, in isolated canine ventricular cardiomyocytes and human induced pluripotent stem cells (iPS)-derived cardiomyocytes, LUF7244 remarkably shortened the APD$_{90}$, which is in line with its activator characteristics (Qile et al., 2019). Moreover, we demonstrated that LUF7244 suppressed EADs in isolated canine ventricular myocytes and prevented dofetilide-induced ventricular arrhythmias in the dog with chronic atrioventricular node block (Qile et al., 2019).

In conclusion, the current study demonstrates that LUF7244, and possibly also other negative allosteric modulators and activators, might also have a role in suppression or preventing arrhythmia caused by defective forward trafficking. Thus, the negative allosteric modulator/activator

LUF7244 in combination with a genuine $K_v11.1$ inhibitor could provide a new pharmacological treatment to functionally correct both congenital and acquired $K_v11.1$ trafficking defects.

Authorship Contributions

Participated in research design: Stary-Weinzinger, Delisle, van der Heyden.

Conducted experiments: Qile, Ji, Golden, Houtman, Romunde, Fransen, van Ham.

Contributed to reagents or analytic tools: IJzerman, January, Heitman, Stary-Weinzinger, Delisle.

Performed data analysis: Qile, Ji, Golden, Houtman, van Ham.

Wrote or contributed to the writing of the manuscript: van der Heyden, Ji, Qile, Stary-Weinzinger, Delisle.

References

Abraham M, Hess B, van der Spoel D, and Lindahl E (2015) *USER MANUAL Version 5.0. 7*, The GROMACS Development Teams at the Royal Institute of Technology and Uppsala University, Sweden.

Anderson CL, Delisle BP, Anson BD, Kilby JA, Will ML, Tester DJ, Gong Q, Zhou Z, Ackerman MJ, and January CT (2006) Most LQT2 mutations reduce $K_v11.1$ (hERG) current by a class 2 (trafficking-deficient) mechanism. *Circulation* **113**:365–373.

Anderson CL, Kuzmicki CE, Childs RR, Hintz CJ, Delisle BP, and January CT (2014) Large-scale mutational analysis of $K_v11.1$ reveals molecular insights into type 2 long QT syndrome. *Nat Commun* **5**:5535.

Bossu A, van der Heyden MAG, de Boer TP, and Vos MA (2016) A 2015 focus on preventing drug-induced arrhythmias. *Expert Rev Cardiovasc Ther* **14**:245–253.

Bussi G, Donadio D, and Parrinello M (2007) Canonical sampling through velocity rescaling. *J Chem Phys* **126**:014101.

Casis O, Olesen SP, and Sanguinetti MC (2006) Mechanism of action of a novel human ether-a-go-go-related gene channel activator. *Mol Pharmacol* **69**:658–665.

Christopoulos A, Changeux JP, Catterall WA, Fabbro D, Burris TP, Cidlowski JA, Olsen RW, Peters JA, Neubig RR, Pin JP, et al. (2014) International Union of Basic and Clinical Pharmacology. XC. multisite pharmacology: recommendations for the nomenclature of receptor allosterism and allosteric ligands. *Pharmacol Rev* **66**:918–947.

Cordes JS, Sun Z, Lloyd DB, Bradley JA, Opsahl AC, Tengowski MW, Chen X, and Zhou J (2005) Pentamidine reduces hERG expression to prolong the QT interval. *Br J Pharmacol* **145**:15–23.

Darden T, York D, and Pedersen L (1993) Particle mesh Ewald: an N·log (N) method for Ewald sums in large systems. *J Chem Phys* **98**:10089–10092.

de Git KC, de Boer TP, Vos MA, and van der Heyden MAG (2013) Cardiac ion channel trafficking defects and drugs. *Pharmacol Ther* **139**:24–31.

Dennis AT, Wang L, Wan H, Nassal D, Deschenes I, and Ficker E (2012) Molecular determinants of pentamidine-induced hERG trafficking inhibition. *Mol Pharmacol* **81**:198–209.

Ficker E, Obejero-Paz CA, Zhao S, and Brown AM (2002) The binding site for channel blockers that rescue misprocessed human long QT syndrome type 2 ether-a-gogo-related gene (HERG) mutations. *J Biol Chem* **277**:4989–4998.

Gardner A, Wu W, Thomson S, Zangerl-Plessl EM, Stary-Weinzinger A, and Sanguinetti MC (2017) Molecular basis of altered hERG1 channel gating induced by ginsenoside Rg3. *Mol Pharmacol* **92**:437–450.

Garg V, Stary-Weinzinger A, and Sanguinetti MC (2013) ICA-105574 interacts with a common binding site to elicit opposite effects on inactivation gating of EAG and ERG potassium channels. *Mol Pharmacol* **83**:805–813.

Gerlach AC, Stoehr SJ, and Castle NA (2010) Pharmacological removal of human ether-a-go-go-related gene potassium channel inactivation by 3-nitro-N-(4-phenoxyphenyl) benzamide (ICA-105574). *Mol Pharmacol* **77**:58–68.

Guo J, Cheng YM, Lees-Miller JP, Perissinotti LL, Claydon TW, Hull CM, Thouta S, Roach DE, Durdagi S, Noskov SY, et al. (2015) NS1643 interacts around L529 of hERG to alter voltage sensor movement on the path to activation. *Biophys J* **108**:1400–1413.

Hess B, Bekker H, Berendsen HJC, and Fraaije JGEM (1997) LINCS: a linear constraint solver for molecular simulations. *J Comput Chem* **18**:1463–1472.

Himmel HM (2013) Drug-induced functional cardiotoxicity screening in stem cell-derived human and mouse cardiomyocytes: effects of reference compounds. *J Pharmacol Toxicol Methods* **68**:97–111.

Imai YN, Ryu S, and Oiki S (2009) Docking model of drug binding to the human ether-à-go-go potassium channel guided by tandem dimer mutant patch-clamp data: a synergic approach. *J Med Chem* **52**:1630–1638.

Jo S, Kim T, Iyer VG, and Im W (2008) CHARMM-GUI: a web-based graphical user interface for CHARMM. *J Comput Chem* **29**:1859–1865.

Jones G, Willett P, Glen RC, Leach AR, and Taylor R (1997) Development and validation of a genetic algorithm for flexible docking. *J Mol Biol* **267**:727–748.

Kamiya K, Niwa R, Mitcheson JS, and Sanguinetti MC (2006) Molecular determinants of HERG channel block. *Mol Pharmacol* **69**:1709–1716.

Kuryshev YA, Ficker E, Wang L, Hawryluk P, Dennis AT, Wible BA, Brown AM, Kang J, Chen XL, Sawamura K, et al. (2005) Pentamidine-induced long QT syndrome and block of hERG trafficking. *J Pharmacol Exp Ther* **312**:316–323.

Nalos L, de Boer TP, Houtman MJ, Rook MB, Vos MA, and van der Heyden MAG (2011) Inhibition of lysosomal degradation rescues pentamidine-mediated decreases of $K_{(IR)}2.1$ ion channel expression but not that of $K_{(v)}11.1$. *Eur J Pharmacol* **652**:96–103.

Obergrussberger A, Juhasz K, Thomas U, Stölzle-Feix S, Becker N, Dörr L, Beckler M, Bot C, George M, and Fertig N (2016) Safety pharmacology studies using EFP and impedance. *J Pharmacol Toxicol Methods* **81**:223–232.

Parrinello M and Rahman A (1981) Polymorphic transitions in single crystals: a new molecular dynamics method. *J Appl Phys* **52**:7182–7190.

Perissinotti L, Guo J, Kudaibergenova M, Lees-Miller J, Ol'khovich M, Sharapova A, Perlovich GL, Muruve DA, Gerull B, Noskov SY, et al. (2019) The pore-lipid interface: role of amino-acid determinants of lipophilic access by ivabradine to the hERG1 pore domain. *Mol Pharmacol* **96**:259–271.

Perry M, Sachse FB, and Sanguinetti MC (2007) Structural basis of action for a human ether-a-go-go-related gene 1 potassium channel activator. *Proc Natl Acad Sci USA* **104**:13827–13832.

Perry M, Sanguinetti M, and Mitcheson J (2010) Revealing the structural basis of action of hERG potassium channel activators and blockers. *J Physiol* **588**:3157–3167.

Qile M, Beekman HDM, Sprenkeler DJ, Houtman MJC, van Ham WB, Stary-Weinzinger A, Beyl S, Hering S, van den Berg DJ, de Lange ECM, et al. (2019) LUF7244, an allosteric modulator/activator of $K_v11.1$ channels, counteracts dofetilide-induced torsades de pointes arrhythmia in the chronic atrioventricular block dog model. *Br J Pharmacol* **176**:3871–3885.

Rajamani S, Anderson CL, Anson BD, and January CT (2002) Pharmacological rescue of human $K^{(+)}$ channel long-QT2 mutations: human ether-a-go-go-related gene rescue without block. *Circulation* **105**:2830–2835.

Sala L, Yu Z, Ward-van Oostwaard D, van Veldhoven JP, Moretti A, Laugwitz KL, Mummery CL, IJzerman AP, and Bellin M (2016) A new hERG allosteric modulator rescues genetic and drug-induced long-QT syndrome phenotypes in cardiomyocytes from isogenic pairs of patient induced pluripotent stem cells. *EMBO Mol Med* **8**:1065–1081.

Sanguinetti MC (2014) HERG1 channel agonists and cardiac arrhythmia. *Curr Opin Pharmacol* **15**:22–27.

Sanguinetti MC and Tristani-Firouzi M (2006) hERG potassium channels and cardiac arrhythmia. *Nature* **440**:463–469.

Saxena P, Zangerl-Plessl EM, Linder T, Windisch A, Hohaus A, Timin E, Hering S, and Stary-Weinzinger A (2016) New potential binding determinant for hERG channel inhibitors. *Sci Rep* **6**:24182.

Schrodinger LLC (2015) *The PyMOL Molecular Graphics System, Version 1.8*, Schrodinger LLC, New York.

Torp-Pedersen C, Møller M, Bloch-Thomsen PE, Køber L, Sandøe E, Egstrup K, Agner E, Carlsen J, Videbaek J, Marchant B, et al.; Danish Investigations of Arrhythmia and Mortality on Dofetilide Study Group (1999) Dofetilide in patients with congestive heart failure and left ventricular dysfunction. *N Engl J Med* **341**:857–865.

Vandenberg JI, Perry MD, Perrin MJ, Mann SA, Ke Y, and Hill AP (2012) hERG $K^{(+)}$ channels: structure, function, and clinical significance. *Physiol Rev* **92**:1393–1478.

Vanommeslaeghe K, Hatcher E, Acharya C, Kundu S, Zhong S, Shim J, Darian E, Guvench O, Lopes P, Vorobyov I, et al. (2010) CHARMM general force field: a force field for drug-like molecules compatible with the CHARMM all-atom additive biological force fields. *J Comput Chem* **31**:671–690.

Varkevisser R, Houtman MJ, Linder T, de Git KC, Beekman HD, Tidwell RR, IJzerman AP, Stary-Weinzinger A, Vos MA, and van der Heyden MAG (2013a) Structure-activity relationships of pentamidine-affected ion channel trafficking and dofetilide mediated rescue. *Br J Pharmacol* **169**:1322–1334.

Varkevisser R, Houtman MJ, Waasdorp M, Man JC, Heukers R, Takanari H, Tieland RG, van Bergen En Henegouwen PM, Vos MA, and van der Heyden MA (2013b) Inhibiting the clathrin-mediated endocytosis pathway rescues $K_{(IR)}2.1$ down-regulation by pentamidine. *Pflugers Arch* **465**:247–259.

Wang W and MacKinnon R (2017) Cryo-EM structure of the open human ether-à-go-go-related K+ channel hERG. *Cell* **169**:422–430.e10.

Wible BA, Hawryluk P, Ficker E, Kuryshev YA, Kirsch G, and Brown AM (2005) HERG-Lite: a novel comprehensive high-throughput screen for drug-induced hERG risk. *J Pharmacol Toxicol Methods* **52**:136–145.

Yan M, Zhang K, Shi Y, Feng L, Lv L, and Li B (2015) Mechanism and pharmacological rescue of berberine-induced hERG channel deficiency. *Drug Des Devel Ther* **9**:5737–5747.

Yu Z, Klaasse E, Heitman LH, and IJzerman AP (2014) Allosteric modulators of the hERG $K^{(+)}$ channel: radioligand binding assays reveal allosteric characteristics of dofetilide analogs. *Toxicol Appl Pharmacol* **274**:78–86.

Yu Z, Liu J, van Veldhoven JP, IJzerman AP, Schalij MJ, Pijnappels DA, Heitman LH, and de Vries AA (2016) Allosteric modulation of Kv11.1 (hERG) channels protects against drug-induced ventricular arrhythmias. *Circ Arrhythm Electrophysiol* **9**:e003439.

Yu Z, van Veldhoven JP, 't Hart IM, Kopf AH, Heitman LH, and IJzerman AP (2015) Synthesis and biological evaluation of negative allosteric modulators of the Kv11.1(hERG) channel. *Eur J Med Chem* **106**:50–59.

Zhou Z, Gong Q, and January CT (1999) Correction of defective protein trafficking of a mutant HERG potassium channel in human long QT syndrome. Pharmacological and temperature effects. *J Biol Chem* **274**:31123–31126.

Address correspondence to: M.A.G. van der Heyden, Department of Medical Physiology, DH&L, Yalelaan 50, 3584 CM Utrecht, The Netherlands. E-mail: m.a.g.vanderheyden@umcutrecht.nl